OPA1, the Disease Gene for Autosomal Dominant Optic Atrophy, Is Specifically Expressed in Ganglion Cells and Intrinsic Neurons of the Retina

Ulrike E. A. Pesch,[1] *Julia E. Fries,*[2] *Stefanie Bette,*[1] *Hubert Kalbacher,*[3] *Bernd Wissinger,*[1] *Christiane Alexander,*[4] *and Konrad Kohler*[2]

Purpose. Autosomal dominant optic atrophy is a hereditary disorder characterized by progressive loss of vision and caused by mutations in a dynamin-related gene, *OPA1*, which translates into a protein with a mitochondrial leader sequence. In this study the *OPA1* gene and its protein were localized in the rat and mouse retina, and its rat orthologue, r*Opa1*, was identified.

Methods. The r*Opa1* cDNA was isolated by using reverse transcribed cDNA from total RNA obtained from a rat retinal ganglion cell line. The spatial and temporal expression patterns of *OPA1* and its gene product were investigated by RNA in situ hybridization and immunohistochemistry in mouse and rat retinas. To characterize further the OPA1-positive neurons, retinal ganglion cells were retrogradely labeled by an immunogold fluorescent tracer or double labeled with OPA1 and choline acetyltransferase or calbindin antibodies.

Results. Protein sequence alignment revealed a 96% identity between rat and human *OPA1* mRNA. *OPA1* expression was found as early as postnatal day 3 in the developing rodent retina. In the mature retina, the *OPA1* gene and its protein were found not only in retinal ganglion cells, but also in starburst amacrine cells and horizontal cells, both of which are involved in lateral signal processing within the retina. However, OPA1 was absent from mitochondria rich nerve fibers and photoreceptor indicating a specific role for OPA1 in signal processing rather than in the requirement of mitochondrial energy supply in the retina.

Conclusions. The data suggest an important and specific function of the OPA1 protein, not only in the optic nerve forming ganglion cells but also in the intrinsic signal processing of the inner retina. (*Invest Ophthalmol Vis Sci.* 2004;45:4217–4225) DOI:10.1167/iovs.03-1261

From the Laboratories of [1]Molecular Genetics and [2]Neurohistology and Cell Biology, University Eye Hospital Tübingen, Tübingen, Germany; the [3]Institute of Physiological Chemistry, University of Tübingen, Tübingen, Germany; and the [4]Max Delbrück Center for Molecular Medicine, Berlin, Germany.

Supported by Grant Fö. 01KS9602 from the German Federal Ministry of Education, Science, Research, and Technology; a grant from the Interdisciplinary Center of Clinical Research (IZKF), Tübingen; and Grant Wi 1189/4-1 from Deutsche Forschungsgemeinschaft.

Submitted for publication November 19, 2003; revised June 23, 2004; accepted July 8, 2004.

Disclosure: **U.E.A. Pesch**, None; **J.E. Fries**, None; **S. Bette**, None; **H. Kalbacher**, None; **B. Wissinger**, None; **C. Alexander**, None; **K. Kohler**, None

The publication costs of this article were defrayed in part by page charge payment. This article must therefore be marked "*advertisement*" in accordance with 18 U.S.C. §1734 solely to indicate this fact.

Corresponding author: Konrad Kohler, Laboratory of Neurohistology and Cell Biology, University Eye Hospital Tübingen, Röntgenweg 11, 72076 Tübingen, Germany; konrad.kohler@uni-tuebingen.de.

Autosomal dominant optic atrophy (adOA) of the Kjer type is a hereditary disorder characterized by progressive loss of visual acuity, color vision deficits, central visual field defects, and temporal optic disc pallor, with an insidious onset in early childhood.[1–3] adOA occurs with an estimated prevalence of 1 in 10,000 in Denmark[4] and 1 and 50,000 elsewhere,[5] rendering it the most common form of hereditary optic neuropathy. The high prevalence in Denmark can be attributed to genetic drift of a single founder mutation.[6] This disease exhibits highly variable expression, even within families, and asymptomatic carriers have been observed in some families.[2,7–11] Histopathologic postmortem examination of donor eyes, performed approximately 30 years ago, suggests that the fundamental disease of adOA is caused by primary degeneration of retinal ganglion cells followed by ascending atrophy of the optic nerve.[12,13] Diffuse atrophy of the retinal ganglion cell layer (GCL), in particular from the macular area, with a loss of myelin and nerve tissue within the optic nerves have been described as pathologic changes in one patient.[12] Ultrastructural examination[13] revealed only a few remaining cells in the GCL of the retina, heavy fibrosis, and, in particular, a highly condensed inner limiting membrane. The optic nerve, the optic chiasm, and the optic tracts showed an increased content of collagen tissue and a decreased number of neurofibrils and myelin sheaths. In the lateral geniculate body, a massive loss of ganglion cells, fibrillary gliosis, and a high quantity of fine granular lipid in the cytoplasm of the ganglion cells was found. Both studies did not note any appreciable changes in the remaining retinal layers. These early histologic findings were consistent with the electrophysiological picture: Patients with adOA showed pattern-ERG deficits suggestive of ganglion cell disease.[14–16]

In 2000, we and others identified several mutant forms of the disease gene *OPA1*.[17,18] This gene encodes a dynamin-related guanosine triphosphatase (GTPase) and is composed of 31 exons that are distributed across ~100 kb of genomic DNA on human chromosome 3 at q28-29. Several splice variants were recently reported[19] caused by exclusion or inclusion of exons 4, 4b, or 5b. The full-length open reading frame (ORF) of 3045 bp translates into a predicted protein of 1015 amino acids, with a mitochondrial leader sequence at the N terminus of the protein and a characteristically conserved GTPase domain in the middle. The putative mitochondrial localization was experimentally confirmed by reporter gene analysis and colocalization with Hsp60 in HeLa cells.[18] Most recent findings indicate that the OPA1 protein is anchored to the mitochondrial inner membrane facing the intermembrane space.[20] Northern blot analysis of human RNA showed that *OPA1* transcripts are present in all analyzed tissues but are most abundant in the retina.[17]

Recently, OPA1 immunoreactivity has been described in the mouse retina.[21] However, until now, nothing has been known about the cellular expression and localization of the *OPA1* gene and the identity of the cells containing this protein in the retina. In this study, we demonstrated spatial and temporal

distribution of the *OPA1* mRNA and its protein in the developing rat and mouse retina, as well as the expression pattern of the OPA1 protein in identified and distinct neurons of the adult rat retina. In addition, we report on identification of r*Opa1*, the rat orthologue of *OPA1*. Preliminary results have been published in abstract form (Pesch UEA, et al. *IOVS* 2001;42:ARVO Abstract 3521).

METHODS

Isolation of r*Opa1* cDNA

Total RNA was isolated from a rat retinal ganglion cell line (R28)[10] using extraction reagent (Trizol; Invitrogen-Life Technologies, Eggstein, Germany). To establish the cDNA sequence of the rat orthologue of *OPA1*, r*Opa1*, we synthesized first-strand rat-cDNA from the obtained total RNA (Ready-to-Go cDNA Synthesis kit; Amersham, Freiburg, Germany). Overlapping PCR fragments covering the entire rat *OPA1* ORF were amplified from the generated rat first-strand cDNA with a combination of human and mouse cDNA primers. All PCR products were purified and directly sequenced by cycle sequencing. The raw sequence data were then assembled (DNAStar Sequencing Project Management software; Lasergene, Madison, WI) and the ORF was identified by ORF-Finder (National Center for Biotechnology Information [NCBI], Bethesda, MD).

To develop spliced transcripts, total RNA from the retina and RPE/choroid was isolated (RNeasy Total RNA-Kit; Qiagen, Hilden, Germany). First-strand cDNA was synthesized from 1 μg total RNA, using an oligo d(T)–primed reaction mixture (20 μL) with reverse transcriptase (Superscript RNase H; Invitrogen-Life Technologies Inc., Gaithersburg, MD) according to standard procedures. PCR amplification of r*Opa1* isoforms was performed with the following primer pair: sense primer, 5′-CTC CCG CGT GGC CGT CT-3′, and antisense primer, 5′-GAG TGT GCA GAA GTT CTT CC-3′. All PCR products were directly TA-cloned into pCR2 (Invitrogen, Carlsbad, CA) and sequenced.

In Vitro Transcription and Generation of Riboprobes

To generate the riboprobe, plasmid DNA containing the full-length human *OPA1* cDNA (AB011139; GenBank; http://www.ncbi.nlm.nih.gov/Genbank; provided in the public domain by NCBI, Bethesda, MD) was linearized with either *Not*I (antisense probe) or *Sal*I (sense probe). There is a 88% homology over the ORF on the nucleotide level between the human and rat and a 89% homology between the human and the mouse. For positive control experiments, plasmid DNA containing the rat rhodopsin cDNA (Z46957) was linearized by *Xho*I (sense probe) and *Not*I (antisense probe). The linearized DNA was purified by phenol-chloroform extraction and 1 μg purified linear DNA was used as the template to synthesize digoxygenin-labeled riboprobes (both sense and antisense) by in vitro run-off transcription with incorporation of digoxigenin-UTP (DIG-RNA labeling kit; Roche Diagnostics, Mannheim, Germany). These cRNA probes were finally hydrolyzed to obtain an appropriate probe length of 200 bp.

Antibody Production

To obtain a polyclonal antibody against OPA1, a peptide comprising the sequence ANTLRQQLTNTEVRRLEK (18-mer), which corresponds to amino acids 891-908 (100% conserved between human, rat, and mouse) of the C-terminal domain of the OPA1 protein was prepared by solid-phase peptide synthesis, using the Fmoc/But strategy. A Blast search was performed with the polypeptide sequence, and no other protein in the NCBI database showed any similarity. The peptide was purified by HPLC to a homogeneity of more than 95%, and the identity was confirmed by electrospray mass spectrometry. Each peptide was coupled to keyhole limpet hemocyanin (KLH) by the glutaraldehyde method. A polyclonal antiserum was raised in New Zealand White rabbits, according to standard immunization protocols (Charles River Service Laboratory System, Wilmington, MA). The antiserum was purified by protein Sepharose affinity chromatography and finally concentrated by ultrafiltration on a 20-kDa membrane to a concentration of 1.0 mg/mL.

Western Blot Analysis

Retina and brain tissue from adult rats was homogenized in ice-cold homogenization buffer (20 mM Tris-HCl [pH 7.4], 0.25 M sucrose, 1 mM EDTA, 0.5 g/L BSA, and 100 μM phenylmethylsulfonyl fluoride [PMSF]) supplemented with protease inhibitor (Set III; Calbiochem, Schwalbach, Germany) using standard protocols. HEK 293 cells were incubated at −80°C overnight and then suspended in the homogenization buffer–protease inhibitor cocktail.

All probes were mixed with Laemmli SDS-PAGE sample buffer, boiled for 5 minutes, separated on 10% SDS-polyacrylamide gels, and electrotransferred to nitrocellulose membranes. The membranes were blocked for 1 hour at room temperature with blocking solution (10 mM Tris-HCl [pH 8.0], 150 mM NaCl, 0.05% Tween 20, and 5% skim milk) and incubated overnight at 4°C, either with our own OPA1 antibody (1:500 in blocking solution) or an OPA1 antibody generated by Misaka et al.[22] (1:1000 in blocking solution) against amino acids 938-960 of mouse OPA1. The reaction was visualized with horseradish peroxidase–conjugated secondary antibody and chemiluminescence reagent (ECL Plus; Amersham).

Animals and Tissue Preparation

All experiments performed in this study were in accordance with the ARVO Statement for the Use of Animals in Ophthalmic and Vision Research. Retinas from Brown Norway rats and C57BL/6J mice from postnatal day (P)3 to adult (P76) were used (day of birth was P0). The animals were kept under a 12-hour light–dark cycle, with an illumination of 10 lux. Tissue samples were taken during the light phase between 9 AM and 5 PM.

Animals were killed with CO_2. Eyes were enucleated and hemisected along the ora serrata. The anterior parts with cornea and lens were removed, and the posterior eye cups with the retina in place were fixed in 4% paraformaldehyde (PFA) in phosphate buffer (PB; pH 7.4) for 30 minutes at 4°C. Eye cups were cryoprotected by immersion in 30% sucrose in PB overnight at 4°C and embedded in freezing compound (Cryomatrix; Shandon, Pittsburgh, PA), and 10-μm cryosections were collected on tissue-adhesive–coated (Vectabond; Vector Laboratories, Burlingame, CA; for in situ hybridization) or gelatin-coated (for immunohistochemistry) glass slides.

In Situ Hybridization

Slide-mounted sections were preincubated with proteinase K buffer (PKB: 0.1 M Tris-HCl [pH 8.0] and 0.05 M EDTA [pH 8.0]) at 37°C for 5 minutes and then treated with proteinase K (0.3 μg/mL) in PKB at 37°C for 8 minutes. Slides were washed twice in diethyl pyrocarbonate (DEPC)-H_2O (Sigma-Aldrich; Deisenhofen, Germany), fixed in 4% PFA in 0.2 M PB for 15 minutes, washed again three times, and dried at room temperature for 10 minutes.

The riboprobes were diluted in hybridization buffer (0.2 ng/μL) and heated to 68°C to 72°C for 10 minutes. Probes were applied to the retina sections and slides were incubated for hybridization in a humidified chamber at 62°C to 65°C overnight. Slides were then washed and treated for 30 minutes with blocking solution (10% blocking reagent in 0.1 M maleic acid and 0.15 M NaCl [pH 7.5]) before the incubation with anti-digoxigenin-AP, Fab-fragment antibodies (1:500). The detection reaction was performed out in AP-buffer with 400 μg/mL of both nitroblue tetrazolium chloride and 5-bromo-4-chlor-3-indolylphosphate in a humidified chamber in the dark for 5 to 48 hours at 4°C and then stopped in 0.1 M Tris-HCl and 0.01 M EDTA (pH 8.0; 15 minutes). Positive control experiments were performed with the generated rat rhodopsin riboprobes.

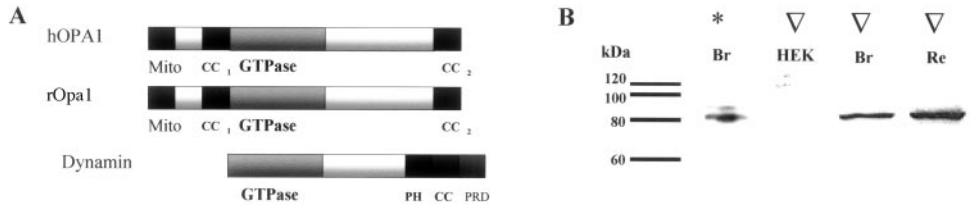

FIGURE 1. Functional protein domains of OPA1 and dynamin and protein expression of OPA1 in the retina. (**A**) Human (h) OPA1, its rat orthologue rOpa1, and dynamin are highly conserved within their GTPase domains. In addition, hOPA1 and rOpa1 contain a mitochondrial leader sequence (Mito) of 85.5% identity and two coiled-coil domains (CC_1, CC_2), whereas dynamin harbors a pleckstrin (PH), one coiled-coil (CC), and a prolin-rich domain (PRD) at its C terminus. (**B**) Western blot analysis of the OPA1 protein in HEK 293 cells (HEK), rat brain (Br), and rat retina (Re). As a standard for specificity of our newly generated antibody, an antibody raised against mOPA1 was used (*asterisk*). The mOPA1 antibody is known from the literature to recognize an OPA1-specific band at 90 kDa in Western blots of brain samples.[22] (▽) Proteins labeled in Western blots by our own polyclonal antibody raised against a peptide in the C terminus of OPA1. HEK cells were used as a negative control. No OPA1 protein was detectable with our antibody in these cells. Brain tissue was used as a positive control. In both rat brain and rat retina, a band is detectable with our OPA1 antibody at a molecular mass of approximately 90 kDa. *Band detected with an antibody directed against a mouse Opa1 sequence. *Left*: Positions of the molecular mass markers.

Immunohistochemistry

Sections were preincubated with 3% H_2O_2 and 40% methanol in phosphate-buffered saline (PBS) to block endogenous peroxidases. The OPA1 antibody was diluted 1:1000 in PBS containing 0.1% TritonX-100 and visualized with a biotinylated secondary antibody (goat anti rabbit; dilution 1:200) and an avidin-biotin peroxidase complex (Vector Laboratories) and diaminobenzidine, in combination with a nickel intensification as a chromogene. For control experiments, the primary antibody was preabsorbed with the antigenic peptide.

Retinal ganglion cells were retrogradely labeled with immunogold fluorescent tracer (Flurogold; Fluorochrome, Englewood, CO) injected into the lateral geniculate nucleus, and sections from these retinas were used for OPA1 immunohistology. For colocalizing OPA1 with choline acetyltransferase (CHAT) or calbindin (CALB), antibodies raised in mouse against CHAT or CALB (Chemicon, Hofheim, Germany) were diluted 1:100 and applied in combination with the OPA1 antibody in the same incubation steps. The appropriate secondary antibodies were conjugated with FITC or Cy3.

All histologic examination and documentation were performed with a multifunction microscope (AX70; Olympus, Tokyo, Japan). Photographs were digitized and adjusted for brightness and contrast (Photoshop; Adobe Systems, Mountain View, CA).

RESULTS

Cloning of the Rat Orthologue *OPA1* cDNA Sequence, r*Opa1*

We established the ORF cDNA sequence of the r*Opa1* orthologue using cDNA reverse transcribed from total RNA that was obtained from a rat retinal ganglion cell line.[23] Based on murine (AB044138; AK004715) and human (AB011139) cDNA sequences, primers were designed and used for isolation of the full-length *rOPA1* cDNA by PCR analysis. Sequence analysis of amplification products and their comparison with the human nucleotide sequence revealed 88% identity for the ORF, showing a high degree of similarity with its human orthologue. The ORF cDNA of the rat gene was found to comprise 2880 bp, encoding a protein of 961 amino acids (AY333988). Protein sequence alignment revealed a 96% identity, with the predicted protein sequence encoded by the human *OPA1* mRNA, with 100% identity for amino acids 207-678. r*OPA1* contains the same three MPP/MIP cleavage consensus sequences RX ↓ (F/L/I)XX(G/S/T)XXXX ↓ that were found in *mOpa1*[22, 24] and the consensus tripartite guanosine triphosphate (GTP)–binding motif needed for phosphate binding (GXXXGKS/T) and coordination of Mg^{2+} (DXXG) nucleotide binding (T/NKXD) and the dynamin sequence signature.[25] Furthermore, two putative coiled-coil regions were also observed (Fig. 1A). Thus, the greatest similarity was found in the region encoding the GTPase domain. Less sequence identity (85.5%) was observed in regions encoding the mitochondrial leader sequence at the N terminus of the protein. However, virtually all previously identified disease-causing missense mutations[17,19,26–28] affect conserved amino acid residues.

Alternatively spliced transcripts were found by using reverse-transcribed cDNA from total rat retina and RPE–choroid RNA. Use of primers located in exons 1 and 6 resulted in multiple PCR products. Sequencing of these alternate OPA1 isoforms revealed the rat to be homologous with human exons 4b (AY660011) and 5b (AY660012). The encoded amino acid sequences showed no significant homology to other proteins in the NCBI database and revealed 77.8% (4b) and 100% (5b) identity to the corresponding human protein sequences.

Western Blot Analysis of rOpa1

Western blot analysis using our own OPA1 antibody (Fig. 1B) showed a molecular mass of ~90 kDa for Opa1 in the rat retina and the brain. In HEK 293 cells, which can be used as the negative for control Opa1,[22] no cross-reactivity with other proteins was detectable with our antibody. To further confirm the antibody's specificity, we analyzed rat brain samples in parallel with the antibody generated by us and an antibody generated by Misaka et al.,[22] directed against a mouse (m)Opa1 sequence. Positive bands were detectable in the blots (Fig. 1B) with both antibodies at the same molecular mass.

Opa1 mRNA Expression in the Developing Rat and Mouse Retina

To determine cell-specific *Opa1* expression in retinal neurons, we performed RNA in situ hybridization on rat (Fig. 2A) and mouse (Fig. 2B) retinal sections by using a human *OPA1* antisense-riboprobe. The staining pattern in both species was the same. The most intense *OPA1* expression occurred in the cell bodies of the GCL, labeling approximately 90% of the cells in the GCL of fully differentiated rat and mouse retinas (Figs. 2A, 2B). Because the GCL of rodents contains a roughly equal amount of ganglion and displaced amacrine cells, we concluded that both of these two cell types express *Opa1*. Labeled cells were also observed in the inner row of the inner nuclear layer (INL). These INL cells were faintly stained (Figs. 2A, 2B) and represented approximately 3% to 4% of the cells in the inner row of the INL.

Control experiments with the *OPA1* cDNA sense probe yielded no detectable signal in either the rat (Fig. 2C) or the mouse retina (data not shown). To verify the specificity of our in situ hybridization protocol, we used an antisense probe derived from rat rhodopsin cDNA (Z46957) as a positive control. The rhodopsin signal was found only in the outer nuclear layer (Fig. 2D). Hybridization with the corresponding rhodop-

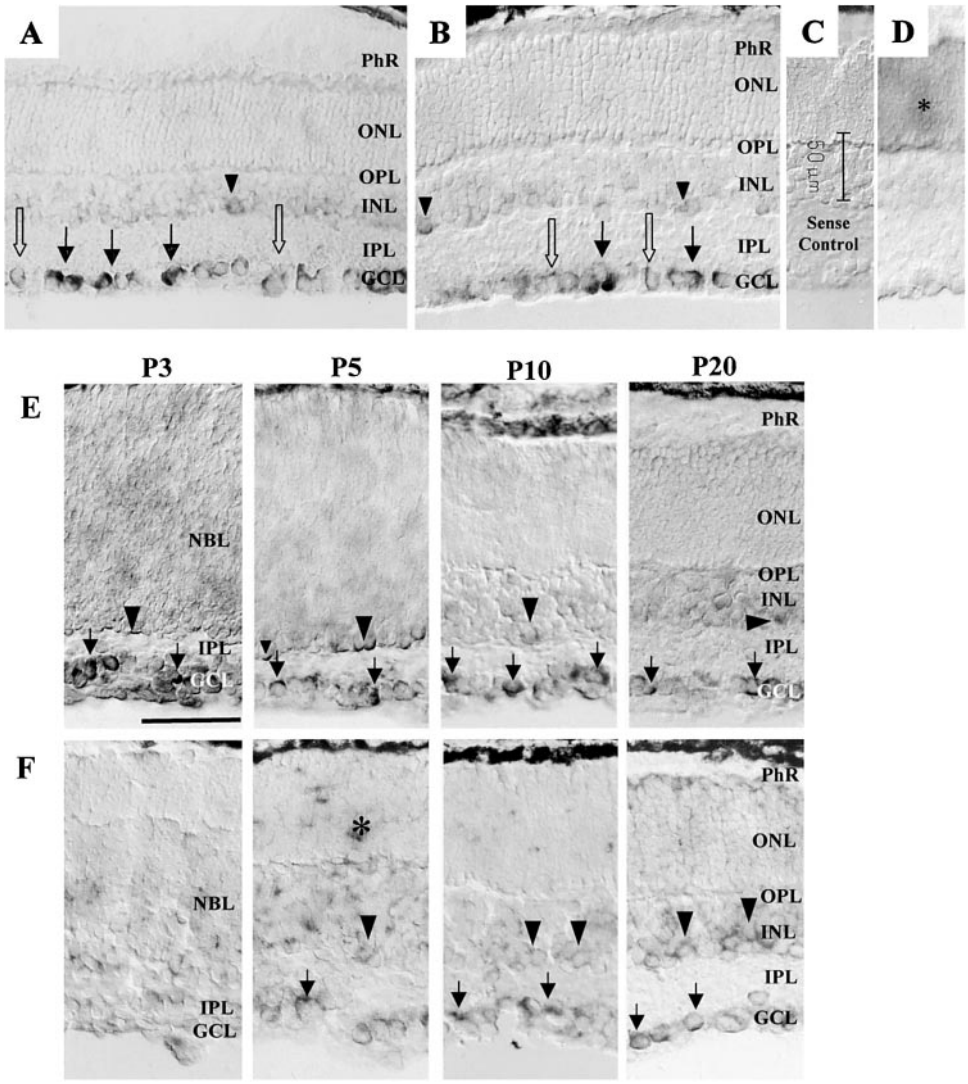

FIGURE 2. Cellular localization of *OPA1* mRNA in the mature and developing rodent retina by in situ hybridization. (**A**) *OPA1* antisense riboprobes in retina radial sections of adult rat and (**B**) mouse. Cells in the GCL (*arrows*) were clearly stained, and cells in the inner half of the INL (*arrowheads*) were occasionally stained. The most intense *OPA1* expression occurred in the cell bodies of the GCL, where, besides these vigorously stained cells (*filled arrows*), cells with a less intense staining (*open arrows*) were present. The outer retina (ONL, PhR) was free of any staining. (**C**) Control experiments with the *OPA1* sense probe did not show any detectable signal over the entire retina. (**D**) To verify the specificity of the in situ hybridization protocol, a rhodopsin antisense probe was used as a positive control. It exclusively labeled the outer retina (✱; ONL of the photoreceptors) leaving the inner retina unstained. (**E**, **F**) Radial sections of rodent retinas at various developmental stages between P3 and P20 hybridized with digoxigenin-labeled *OPA1* riboprobes. In the developing rodent retina only the GCL and the adjacent IPL have already separated from the NBL at P3, with the GCL still being multilayered but in the process of losing its supernumerous cells during the next days of development. (**E**) In the rat retina, at P3 and P5, a clear *OPA1* expression was present in cell bodies of the multilayered GCL (*arrows*) and in the proximal cytoplasm of cells located in the undifferentiated NBL along the IPL border (*arrowheads*). At P10, when the INL is completely separated from the photoreceptors, staining was confined to the GCL and the innermost row of the INL. This staining pattern then persisted in all later developmental stages. (**F**) In the developing mouse retina, the staining pattern was essentially the same as in rats. There was a slight temporal delay in *OPA1* expression, which is consistent with the slower retinal development in the mouse compared with the rat—very faint, if any, positive reaction was visible before P5. Up to P10, there was a tendency for reaction deposits to be randomly scattered over the entire retina, including the outer layers (P5, ✱). Scale bar, 50 μm.

sin sense probe was completely free of any signal (data not shown).

In the developing rat (Fig. 2E) and mouse (Fig. 2F) retinas at P3, only the GCL and the adjacent inner plexiform layer (IPL) had already separated from the neuroblast layer (NBL). The GCL was still multilayered but was in the process of losing its supernumerous cells during the next days of development. At that stage, cells stained positive for *OPA1* within all rows of the multilayered GCL in the rat. In addition, small stripes of labeled cytoplasm were present in the most apical part of some cells in the undifferentiated NBL located just along its inner border (Fig. 2E). Thus, the in situ hybridization pattern was already generally the same in this early postnatal age as in the mature retina. The P5 retina showed the same cellular distribution as at P3 (Fig. 2E). At P10, when the INL was separated from the outer parts of the retina, staining was clearly confined to the GCL and the inner row of the INL (Fig. 2E). There was no alteration in the pattern and intensity of *OPA1* staining after eye opening, which occurs in rats and mice at ~P15 (Fig. 2E; P20).

Even though *OPA1* staining was generally the same for rats (Fig. 2E) and mice (Fig. 2F), its onset was delayed in mice, with no obvious positive staining before P5 (Fig. 2F). Up to P10, there was a tendency for reaction deposits to be randomly scattered over the entire retina, including the outer layers (Fig. 2F).

OPA1 Protein Distribution in the Mouse and Rat Retina

To examine cell-specific protein localization, we performed immunohistochemistry on postnatal rat (Fig. 3A) and mouse (Fig. 3B) retina sections, with polyclonal anti-OPA1 antiserum directed against the C-terminal part of OPA1, which is 100% conserved among human, rat, mouse, and salmon.

OPA1 immunoreactivity was present in both rat and mouse retinas as early as P3, and the time course of protein expression mirrored in general that of the mRNA expression known from the in situ hybridization experiments. However, whereas protein labeling was clearly visible in the mouse at P3 (Fig. 3B), no mRNA was detectable at that developmental stage (Fig. 2F), presumably because of an mRNA level that is beyond the detection limit of the in situ hybridization method. Cells located approximatively in the middle of the NBL were already

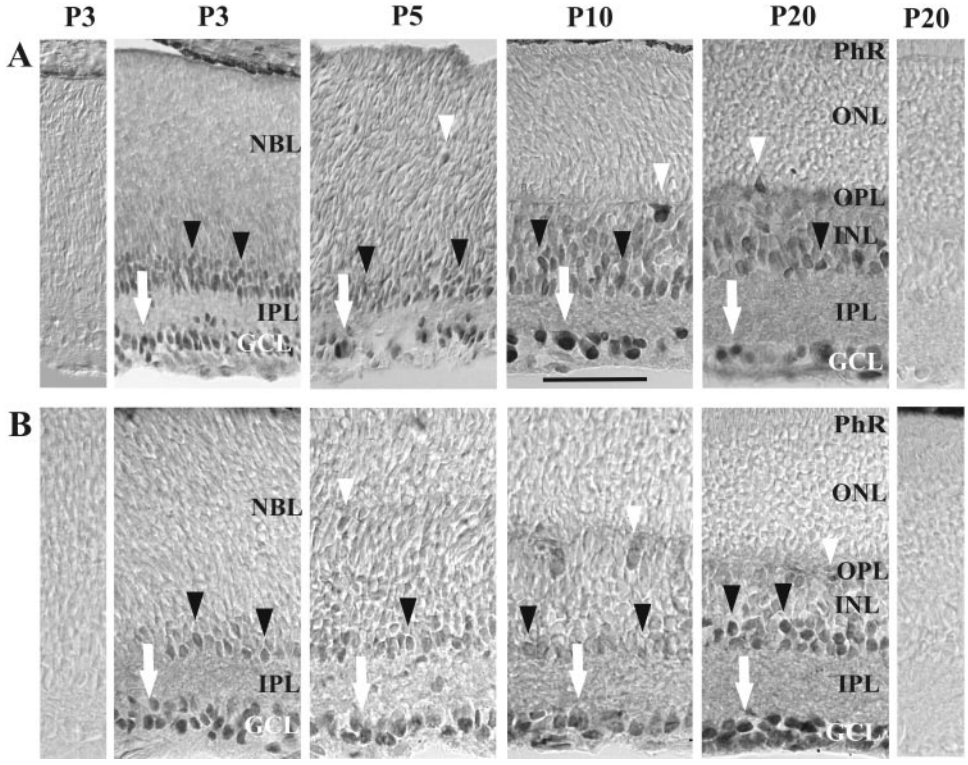

FIGURE 3. Cellular localization with a polyclonal antibody of the OPA1 protein in developing rat (**A**) and mouse (**B**) retinas. Cells were labeled in the GCL (*arrows*) and along the upper border of the IPL (*black arrowheads*) from P3 on in both species. There were stained cells in the middle of the NBL (*white arrowheads*) at P5 and along the INL–OPL border from P10 on (*white arrowheads*). The preabsorbed antibody resulted in a complete absence of immunoreactivity over the entire retina (images to the *left* and *right* of each row). Scale bar, 50 μm.

immunoreactive at ~P5 (Fig. 3B, white arrowheads) and OPA1-positive cells were subsequently found in the outermost row of the INL, adjacent to the outer plexiform layer (OPL) as soon as the OPL had formed and the INL was separated from the outer nuclear layer (ONL) at P10 (Fig. 3B, white arrowheads). Cell label resembling that in an adult retina was achieved at the end of the third postnatal week in both mice and rats (Fig. 3).

In the mature rat retina, strong staining of most of the neurons in the GCL was observed (Figs. 4A, 4B), with approximatively 10% to 15% of unlabeled cell bodies. In agreement with in situ hybridization experiments, cell bodies in the innermost row were stained (Fig. 4B). These were classified as amacrine cells because of their position along the INL/IPL border. In contrast to the in situ hybridization results, we found immunoreactive cells in the outermost row of the INL (Fig. 4B). These were easily identified as horizontal cells, because of their position and elongated horizontal shape. In addition, OPA1 immunoreaction was visible in horizontal processes in the OPL (Fig. 4B) and in two narrow stratified bands in the IPL (Fig. 4B) that were connected to cells in the INL (Figs. 4D, 5B), and GCL (Figs. 4E, 5C), respectively (see also OPA1 immunoreactivity in Fig. 5).

The fiber layer built by the ganglion cell axons and the optic nerve itself remained without any OPA1 immunoreactivity (Fig. 4A). This also holds true for the entire photoreceptor layer, where cell bodies in neither the ONL nor the inner or outer segments of photoreceptors were positive for OPA1.

Control experiments omitting the first antibody or preabsorbing the antiserum with the purified OPA1 protein used for antibody production (Fig. 4C) resulted in a complete absence of immunoreactivity over the entire retina.

To characterize further the OPA1-positive neurons, sections from retinas with ganglion cells retrogradely labeled with immunogold fluorescent tracer (Fluorogold; Fluorochrome) were used or retinal sections were double-labeled with the OPA1 antibody and antibodies directed either against CHAT, known to be specifically expressed in starburst amacrine cells, or calbindin (CALB), a marker for horizontal cells (Fig. 5). OPA1 immunoreactivity was found in all ganglion cells stained by immunogold deposits (Fig. 5A, arrows); however, OPA1-positive cells that showed no colocalization of the gold deposits were also noted in the GCL, indicating the presence of OPA1 also in displaced amacrine cells (Fig. 5A, arrowheads). Double labeling of OPA1 and CHAT revealed that all CHAT-positive amacrine cells in the inner row of the INL as well as CHAT-positive displaced amacrine cells in the GCL coexpressed both proteins (Fig. 5B, arrows in the INL, arrowheads in the GCL). In contrast, some of the OPA1-positive amacrine cells in the INL did not necessarily coexpress CHAT (Fig. 5B3). Processes of CHAT- and OPA1-positive neurons terminated in the same two sublayers of the IPL, and double labeling was observed in both bands (Fig. 5B, asterisks). There was a slightly broader band that occasionally seemed to consists of two layers of processes running in close proximity at sublayer 2 (Figs. 5B2, 5B3, single asterisk) and a finer and more distinct band at sublayer 4 (Figs. 5B2, 5B3, double asterisks). Horizontal cells were identified with an antibody directed against CALB. All CALB-positive processes in the OPL and all cell bodies stained in the outermost row of the INL colocalized with the OPA1 expression in this region of the retina (Fig. 5C, arrowheads).

DISCUSSION

Different mutations in the *OPA1* gene have been identified as causes of autosomal dominant optic atrophy,[6,17,18,26,27] and our previous data have shown a strong *OPA1* expression in homogenates of the human retina.[17] We successfully isolated the rat orthologue of human *OPA1*, r*Opa1*, as well as the alternatively spliced exons 4b and 5b. The predicted 960-amino-acid sequence revealed a similar functional domain composition and a high degree of conservation in the human OPA1 protein (96%). The amino acid sequences of the rat exons 4b and 5b, located between the mitochondrial leader sequence and the GTPase domain, corresponds to a part of the protein with unknown function. They show an identity of 77.8% for 4b

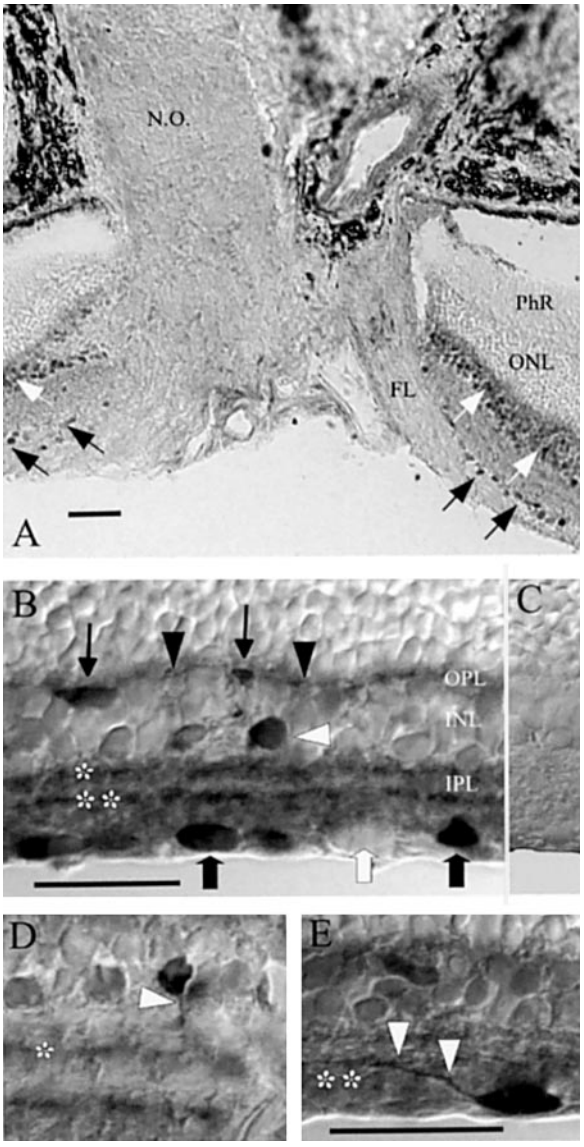

FIGURE 4. Cellular localization of the OPA1 protein in the mature rat retina by immunohistochemistry. (**A**) Radial section through the optic nerve and the adjacent retina. Staining was clearly visible in cells of the GCL (*black arrows)*, with most of the cells labeled, as well as in the INL (*white arrows*). Neither the fiber layer (FL) and the optic nerve (NO), both formed by the ganglion cell axons, nor the outer parts of the retina, consisting of the light-sensitive photoreceptor cells (ONL, PhR), showed any detectable immunoreactivity. (**B–E**) Micrographs of the inner parts of the retina (OPL–GCL). (**B**) Horizontal cells localized along the INL–OPL border (*arrows*) and their thin horizontally running processes in the OPL (*black arrowheads*) were stained by the OPA1 antibody. Within the INL, cells in the innermost row bordering the IPL were immunoreactive (*white arrowhead*). Dividing the IPL into five sublayers, stained bands can be attributed to sublayers 2 (*asterisk*) and 4 (*double asterisks*). OPA1-immunoreactive cells in the GCL (*bold black arrows*); unlabeled cell (*bold white arrow*). (**C**) Control experiments with the preabsorbed antibody resulted in a complete absence of immunoreactivity over the entire retina. (**D**) A descending process (*arrowhead*) originating from an OPA1-positive cell in the INL was connected to the immunoreactive band (*asterisk*) in sublayer 2. (**E**) An ascending process (*arrowheads*) originating from an OPA1-positive cell in the GCL was connected to the immunoreactive band (*double asterisks*) in sublayer 4. Scale bar, 50 μm.

and 100% for 5b, when compared with their human counterparts. All hitherto identified missense mutations in patients bearing *OPA1* affect conserved amino acids. There are also known homologues from other species; however, their similarity to the human OPA1 protein is less than the 96% of the rat homologue (e.g., *Xenopus laevis* [XI20595] 80.11%; *Drosophila* [CG8479] 54%; *Caenorhabditis elegans* [D2013.5] 56%). The high congruence between human and rodent OPA1 expression is further stressed by the fact that we were able to localize rat RNA with the human OPA1 cDNA probe. The mouse and rat animal models will therefore be of great promise for gaining detailed insight into the pathophysiology of OPA1.

As a step toward characterizing the underlying pathophysiology of adOA, we investigated temporal and spatial *Opa1* gene expression patterns during rat and mouse retina development. Our in situ hybridization data convincingly demonstrated that the *Opa1* gene is specifically expressed in the GCL and occasionally in cells in the INL of both rat and mouse retinas. To us, this invariable presence of *Opa1* in the retina indicates a fundamental need of retinal ganglion cells for *Opa1* throughout the entire postnatal lifespan. These findings concur with the histologic investigations of eyes from donors who have had adOA that suggest that the fundamental pathologic characteristic of adOA is a primary degeneration of retinal ganglion cells.[12,13] Besides ganglion cell degeneration, these first and early histopathologic examinations did not reveal any appreciable changes in the remaining retinal layers.

Our immunohistochemical data further confirmed the presence of the OPA1 protein in the GCL and the INL, leaving the photoreceptors and the optic nerve free of any staining. They are also in accordance with recent observations from the developing mouse retina[21] which revealed first OPA1 immunoreactivity already in the undifferentiated neuroblast layer at embryonic day 16.

Furthermore, colocalization experiments showed that OPA1 is present in nearly all if not all RGCs and that CHAT-positive ganglion cells in the INL and GCL are additional sources of *Opa1* expression. These CHAT-containing amacrine cells are starburst cells, which are very particular, in that they occur as two mirror-symmetric layers of cells with cell bodies located in the INL and GCL.[28] CHAT cells located in the INL belong to the OFF amacrine cells, whereas those displaced to the GCL are ON amacrine cells.[29] Whereas all the CHAT-positive cells in the INL and in the GCL express OPA1, the OPA1-positive amacrine cells in the INL do not necessarily do so. Starburst amacrine cells have been known for quite some time to be involved in the visual phenomenon of directional selectivity and connect with cone bipolar cells, other amacrine cells, and direction-selective (DS) ganglion cells.[30] Experiments in transgenic mice with a specific ablation of starburst amacrine cells showed starburst cells to be the key players in the DS light response of ganglion cells.[31] DS information is transmitted to the magnocellular layers in the lateral geniculate nucleus. We would expect such a transmission to be impaired in adOA patients, because of malfunctional OPA1 protein causing a loss of starburst amacrine cells. This would then contrast with findings that visual transmission to the parvocellular rather than to the magnocellular zone is affected in adOA patients. Future work will reveal the exact contribution of starburst cells to directional selectivity in vision and the underlying signaling circuits involving this particular cell population.

To our surprise, horizontal cells were strongly positive for OPA1 staining. This indicates for the very first time a possible role of this cell type in the pathologic course of adOA. A loss of horizontal cells would have remained unnoticed in sections of donor eyes of adOA patients, because of the numerous cell bodies in the INL. Also, electrophysiological examinations, such as ERG recordings, are unsuitable for the detection of horizontal cell loss of function. Horizontal cells can be divided into at least two types: Dendritic processes of type I horizontal cells contact M- and L-cones, whereas type II horizontal cells

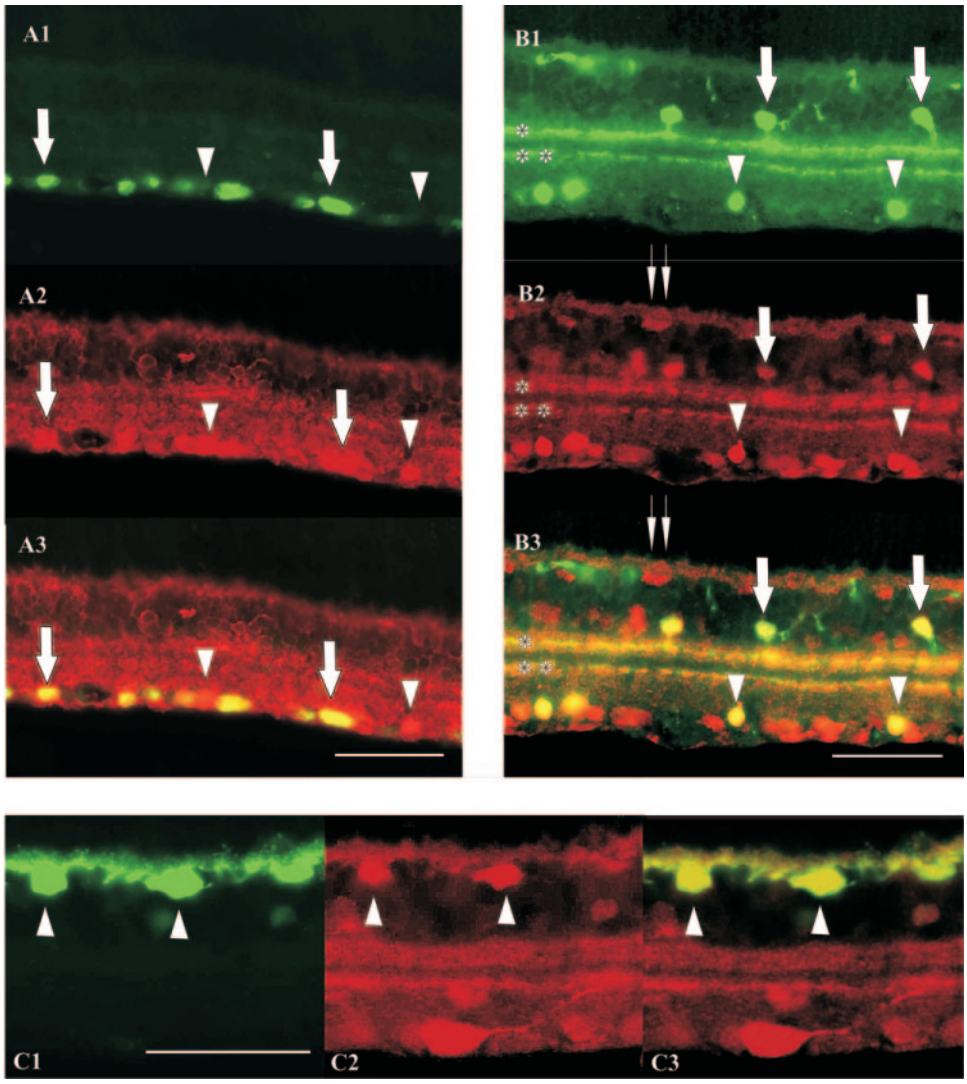

FIGURE 5. Characterization of OPA1-expressing cell types in the GCL and INL. (**A1**) Ganglion cells retrogradely labeled by gold immunolabel (*arrows*); GCL cells that remained without immunogold labeling (*arrowheads*); (**A2**) cells in the GCL immunoreactive for OPA1 (*arrows*, *arrowhead*); (**A3**) merged image of (**A1**) and (**A2**) with colocalization of immunogold and OPA1 in ganglion cells appearing *yellow* (*arrows*). OPA1-positive displaced amacrine cells showed no colocalization of both markers (*arrowheads*). (**B1**) CHAT-positive amacrine cells in the INL (*arrows*) and GCL (*arrowheads*) and their processes in sublayers 2 (*single asterisk*) and 4 (*double asterisks*); (**B2**) cells in the INL (*arrows*) and GCL immunoreactive for OPA1 (*arrowheads*); OPA1-positive bands in the IPL (*asterisks*), with staining along the INL–OPL border (*double arrows*); (**B3**) merged image of CHAT- and OPA1-stained cells in (**B1**) and (**B2**); colocalization appears *yellow* and was present in all cell bodies (*arrows*) in the INL and in the two bands (*asterisks*) in the IPL. Cell bodies in the GCL are either double labeled (*arrowheads*) or remained free of coexpression. (**C1**) CALB-positive horizontal cells in the distal INL (*arrowheads*); (**C2**) OPA1-positive cells in the distal INL (*arrowheads*); (**C3**) merged image of CALB- and OPA1-stained cells in (**C1**) and (**C2**); colocalization appeared *yellow* and was present in all horizontal cells along the INL–OPL border (*arrowheads*) and in horizontal cell processes in the OPL. Scale bar, 50 μm.

make extensive contacts with S-cones, but only sparse contact with M- and L-cones.[32] Moreover, the latter type is not interconnected through gap junctions as is type I. It is striking that one very characteristic symptom, and often the very first one that is objectively measurable in adOA patients is a color vision disturbance.[33] In many cases, a tritan color defect precedes a later total color disturbance. It has been speculated that the tritan color defect is attributable to a loss of RGCs. Now, however, our results point to a possible involvement of horizontal cells. Type II horizontal cells in particular seem to contribute directly to the integration of color visual information of blue components and are excellent candidates for being accountable for this clinical feature. From a clinical viewpoint, we hope that our results will trigger fresh ideas for psychophysical testing of visually impaired patients, such as those affected with adOA. Very first multifocal ERG recordings from the macular region of patients with optic atrophy showed alterations attributable to pathologic alterations in the inner retina (Leo-Kottler B, personal communication, 2003).

Concerning the presence of OPA1 in the horizontal cells, we have to consider that only the protein, not the mRNA, was detected in this cell type. A similar phenomenon was observed in early postnatal stages of the mouse retina. *Opa1* mRNA levels in the horizontal cells below the detectable threshold of in situ hybridization and paralleled by accumulation of the protein may serve as an explanation for this discrepancy in expression profile obtained by the two methods. However, cross-reactivity of the antibody (which then has to be very specific for the horizontal cells) cannot be completely ruled out, even though the carefully examined specificity of the antiserum and the consistency of mRNA and protein expression in amacrine and ganglion cells argue against this.

OPA1 is imported into mitochondria,[22] where it is possibly anchored to the mitochondrial inner membrane facing the intermembrane space.[20] Mitochondrial biogenesis occurs in the somata of the retinal ganglion cells before they are transported to the synaptic terminals through the axons of the optic nerve.[34,35] After myelination of the optic nerve axons posterior to the lamina cribrosa, the number of mitochondria drastically decreases.[36] In addition, the inner segments of photoreceptor cells as well as the fiber layer have the greatest energy demand and contain the most mitochondria within the retina. Therefore, we expected to find OPA1 staining at least anterior to the lamina cribrosa and in the inner segments of the photoreceptors. However, both structures did not show any detectable signal for OPA1. This drastically differs from cyclo-oxygenase (COX) and serine dehydrase (SDH) activity measured in these and other layers in the human retina which have the requirement of mitochondrial energy supply. Thus, we can exclude OPA1 as an important regulator of the provision of adenosine triphosphate (ATP) generated through the respiratory chain. This may highlight a fundamental difference in the primary

disease mechanism of adOA versus Leber's hereditary optic neuropathy (LHON). The origin of disease in LHON is an impairment of complex I in the respiratory chain due to mutations in mitochondrially encoded reduced nicotinamide adenine dinucleotide dehydrogenase (NADH).[37] Because OPA1 is clearly not present in mitochondria of the fiber layer and photoreceptors, it must be involved in other features of the mitochondrial cell biology. Especially the manifestation of disease symptoms in very early childhood and the early expression (at least at P3) of *Opa1* mRNA in the developing rat retina convince us that a developmental defect in adOA should be proposed. Starburst amacrine cells, for instance, form the first identified network of internal neurons that directly participate in spontaneous rhythmic activities in the developing retina.[38] These electrical waves depend on changes in intracellular neurotransmitter, ion, or second-messenger concentrations, which are partly known to be stored in mitochondria. OPA1 is a member of the protein family of large dynamin-related GTPases that are functionally specialized in fission and fusion events in membranes and vesicles.[25,39] Recent studies have reported that mutant OPA1 protein affects mitochondrial morphology, altering it from the standard tubular to a vesicular shape.[22,40] We hypothesize that OPA1 regulates or controls the release of mitochondrial cisternae, such as $FeCa^{2+}$ stores. Neurons, which depend on proper buffering capabilities for Ca^{2+} during development, would be particularly at risk for the excitotoxic effects of mutant OPA1 protein.

The first evidence of possible *OPA1* involvement in related diseases has been established by genetic testing of patients with normal-tension glaucoma (NTG) for genetic variations in the *OPA1* gene.[41] In contrast, no *OPA1* mutations have been identified in any patients with LHON.[27] The design of suitable animal models for adOA and related diseases has to be a next step in the process of conquering these disorders, because human donor tissue material is unavailable to the extent needed for appropriate research concerning the function of *OPA1* as a disease gene. The cloning of the rat sequence in this study is a prerequisite for the generation of a rat model for adOA. In this context, the newly generated OPA1antibody will serve as a valuable tool for further investigation, especially in light of the fact that due to the 100% conservation of its target epitope, this antibody can be used in many different species.

Acknowledgments

The authors thank Armin Huber for providing the rat rhodopsin cDNA clone, Gail M. Seigel for the rat ganglion cell line, Yoshihiro Kubo for generously relinquishing the anti-mOPA1 antibody; Oliver Biehlmaier and German Pinzon-Duarte for fruitful discussions; and Gudrun Haerer for excellent technical assistance.

References

1. Jaeger W. Dominant vererbte Optikusatrophie. *Albrecht v Graefes Arch Ophthalmol*. 1954;155:457–484.
2. Hoyt CS. Autosomal dominant optic atrophy: a spectrum of disability. *Ophthalmology*. 1980;87:245–251.
3. Votruba M, Moore AT, Bhattacharya SS. Clinical features, molecular genetics and pathophysiology of dominant optic atrophy. *J Med Genet*. 1998;35:793–800.
4. Kjer B, Eiberg H, Kjer P, Rosenberg T. Dominant optic atrophy mapped to chromosome 3q region. *Acta Ophthalmol Scand*. 1996;74:3–7.
5. Lyle WM. *Genetic Risks.* Waterloo, Ontario, Canada: University of Waterloo Press; 1990.
6. Thiselton DL, Alexander C, Morris A, et al. A frameshift mutation in exon 28 of the OPA1 gene explains the high prevalence of dominant optic atrophy in the Danish population: evidence for a founder effect. *Hum Genet*. 2001;109:498–502.
7. Caldwell JBH., Howard RO, Riggs LA. Dominant juvenile optic atrophy. *Arch Ophthalmol*. 1971;85:133–147.
8. Kline LB, Glaser JS. Dominant optic atrophy: the clinical profile. *Arch Ophthalmol*. 1979;97:1680–1686.
9. Roggeveen HC, de Winter AP, Went LN. Studies in dominant optic atrophy. *Ophthalmic Paediatr Genet*. 1985;5:103–109.
10. Votruba M, Fitzke FW, Holder GE, Carter A, Bhattacharya SS, Moore AT. Clinical features in affected individuals from 21 pedigrees with dominant optic atrophy. *Arch Ophthalmol*. 1998;116:351–358.
11. Johnston RL, Seller MJ, Behnam JT, Burdon MA, Spalton DJ. Dominant optic atrophy: refining the clinical diagnostic criteria in light of genetic linkage studies. *Ophthalmology*. 1999;106:123–128.
12. Johnston PB, Gaster RN, Smith VC, Tripathi RC. A clinicopathologic study of autosomal dominant optic atrophy. *Am Ophthalmol*. 1979;88:868–875.
13. Kjer P, Jensen OA, Klinken L. Histopathology of eye, optic nerve and brain in a case of dominant optic atrophy. *Acta Ophthalmol*. 1983;61:300–312.
14. Harding GF, Crews SJ, Pitts SM. Psychophysical and visual evoked potential findings in hereditary optic atrophy. *Trans Ophthalmol Soc UK*. 1979;99:96–102.
15. Holder GE, Votruba M, Carter AC, Bhattacharya SS, Fitzke FW, Moore AT. Electrophysiological findings in dominant optic atrophy (DOA) linking to the *OPA1* locus on chromosome 3q 28-qter. *Doc Ophthalmol*. 1998;95:217–228.
16. Berninger TA, Jaeger W, Krastel H. Elektrophysiology and colour perimetry in dominant infantile optic atrophy. *Br J Ophthalmol*. 1991;75:49–52.
17. Alexander C, Votruba M, Pesch UEA, et al. *OPA1*, encoding a dynamin-related GTPase, is mutated in autosomal dominant optic atrophy linked to chromosome 3q28. *Nat Genet*. 2000;26:211–215.
18. Delettre C, Lenaers G, Griffoin JM, et al. Nuclear gene *OPA1*, encoding a mitochondrial dynamin-related protein, is mutated in dominant optic atrophy. *Nat Genet*. 2000;26:207–210.
19. Delettre C, Griffoin JM, Kaplan J, et al. Mutation spectrum and splicing variants in the *OPA1* gene. *Hum Genet*. 2001;109:584–591.
20. Olichon A, Emorine LJ, Descoins E, et al. The human dynamin-related protein OPA1 is anchored to the mitochondrial inner membrane facing the inter-membrane space. *FEBS Lett*. 2002;523:171–176.
21. Aijaz S, Erskine L, Jeffery G, Bhattacharya SS, Votruba M. Developmental expression profile of the optic atrophy gene product: OPA1 is not localized exclusively in the mammalian retinal ganglion cell layer. *Invest Ophthalmol Vis Sci*. 2004;45:1667–1673.
22. Misaka T, Miyashita T, Yoshihiro K. Primary structure of a dynamin-related mouse mitochondrial GTPase and its distribution in brain, subcellular localization, and effect on mitochondrial morphology. *J Biol Chem*. 2002;277:15834–15842.
23. Seigel GM. Establishment of an E1A-immortalized rat retinal cell culture. *In Vitro Cell Dev Biol*. 1996;32:66–68.
24. Branda SS, Cavadini P, Adamec J, et al. Yeast and human frataxin are processed to mature form in two sequential steps by the mitochondrial processing peptidase. *J Biol Chem*. 1999;274:22763–22769.
25. Guan K, Farh L, Marshall TK, Deschenes RJ. Normal mitochondrial structure and genomic maintenance in yeast requires the dynamin-like product of the MGM1 gene. *Curr Genet*. 1993;24:141–148.
26. Pesch UEA, Leo-Kottler B, Mayer S, et al. *OPA1* mutations in patients with autosomal dominant optic atrophy and evidence for semi-dominant inheritance. *Hum Mol Genet*. 2001;10:1359–1368.
27. Toomes C, Marchbank NJ, Mackey DA, et al. Spectrum, frequency and penetrance of *OPA1* mutations in dominant optic atrophy. *Hum Mol Genet*. 2001;10:1369–1378.
28. Jeon CJ, Strettoi E, Masland RH. The major cell populations of the mouse retina. *J Neurosci*. 1998;18:8936–8946.
29. Chalupa LM, Gunhan E. Development of On and Off retinal pathways and retinogeniculate projections. *Prog Retin Eye Res*. 2004;23:31–51.
30. Rodieck RW. *The First Steps in Seeing.* Sunderland, MA: Sinauer Associates; 1998.

31. Yoshida K, Watanabe D, Ishikane H, Tachibana M, Pastan I, Nakanishi S. A key role of starburst amacrine cells in originating retinal directional selectivity and optokinetic eye movement. *Neuron*. 2001;30:771–780.
32. Ahnelt P, Kolb H. Horizontal cells and cone photoreceptors in human retina: a Golgi-electron microscopic study of spectral connectivity. *J Comp Neurol*. 1994;343:406–427.
33. Del Porto G. Clinical heterogeneity of dominant optic atrophy: the contribution of visual function investigations to diagnosis. *Graefes Arch Clin Exp Ophthalmol*. 1994;232:717–727.
34. Grafstein B. Intracellular traffic in nerve cells. *Brain Res Bull*. 1999;50:311–312.
35. Chada SR, Hollenbeck PJ. Mitochondrial movement and positioning in axons: the role of growth factor signaling. *J Exp Biol*. 2003;206:1985–1992.
36. Andrews RM, Griffiths PG, Johnson MA, Turnbull DM. Histochemical localisation of mitochondrial enzyme activity in human optic nerve and retina. *Br J Ophthalmol*. 1999;83:231–235.
37. Carelli V, Ross-Cisneros FN, Sadun AA. Mitochondrial dysfunction as a cause of optic neuropathies. *Prog Retin Eye Res*. 2004;23:53–89.
38. Zhou ZJ. Direct participation of starburst amacrine cells in spontaneous rhythmic activities in the developing mammalian retina. *J Neurosci*. 1998;18:4155–4165.
39. Pelloquin L, Belenguer P, Menon Y, Ducommun B. Identification of a fission yeast dynamin-related protein involved in mitochondrial DNA maintenance. *Biochem Biophys Res Commun*. 1998;251:720–726.
40. Olichon A, Baricault L, Gas N, et al. Loss of OPA1 perturbates the mitochondrial inner membrane structure and integrity, leading to cytochrome c release and apoptosis. *J Biol Chem*. 2003;278:7743–7746.
41. Aung T, Ocaka L, Ebenezer ND, et al. A major marker for normal tension glaucoma: association with polymorphisms in the *OPA1* gene. *Hum Genet*. 2002;110:2–6.